The PHILIPPINE JOURNAL OF Veterinary Medicine

(Original Research)

Histomorphometric and Immunohistochemical Characterization of Hepatic Cirrhosis in Algerian Dromedary Camels (*Camelus dromedarius*)

Allaoua Chaouki Bentazir[1,a,], and Djallal Eddine Rahmoun[2,b]*

[1]Laboratory of Science and Techniques for Living, Institute of Agricultural and Veterinary Sciences Taoura, Mohamed-Cherif Messaadia University - Souk Ahras, BP 41000 Souk-Ahras, Algeria
[2]Laboratory of Animal Production, Biotechnologies and Health (PABIOS): Institute of Agriculture and Veterinary Sciences Taoura, Mohamed-Cherif Messaadia University - Souk Ahras, BP 41000 Souk-Ahras, Algeria

*Corresponding Author: demazir133@gmail.com (Allaoua Chaouki Bentazir)

ORCID Numbers: [a]0000-0001-7785-8847 [b]0000-0001-6723-4491

Submitted: 24 Oct. 2025 Revised: 13 Jan. 2026 Accepted: 25 Mar. 2026 Published: 19 May 2026

Abstract

Background: The dromedary camel is a socio-economically important species in arid regions, and hepatic cirrhosis represents a major threat to its health and productivity. Despite its clinical relevance, a comprehensive pathomorphological description of cirrhosis in this species has been lacking. **Methods**: Liver samples from 24 adult dromedary camels (both sexes, aged approximately 6–12 years), with gross lesions suggestive of cirrhosis and 24 age-matched healthy controls were collected from an abattoir in El Oued, Algeria. Histochemical stains (H&E, Azan trichrome) and immunohistochemical markers for macrophages (CD68) and activated myofibroblasts (α-SMA) were applied. Quantitative histomorphometric analysis was conducted to determine tissue composition. **Results**: Macroscopically, cirrhotic livers showed a significant reduction in mass (8.12 ± 1.86 kg to 6.30 ± 1.25 kg, $p < 0.01$), accompanied by marked nodularity and a firm consistency. Histologically, normal hepatic architecture was replaced by fibrous septa and regenerative nodules. Immunohistochemistry confirmed increased $CD68^+$ macrophages and $\alpha\text{-SMA}^+$ stellate cells in fibrotic areas. Morphometric analysis demonstrated a marked increase in the volume density (Vv) of connective tissue (33.25 ± 2.31% vs. 7.25 ± 2.65%, $p < 0.001$) accompanied by a significant reduction in the Vv of hepatocyte (54.34 ± 4.24% vs. 82.64 ± 4.87%, $p < 0.001$) in cirrhotic livers compared with controls. **Conclusions**: This study provides the first quantitative immunomorphometric characterization of hepatic cirrhosis in Algerian dromedary camels and establishes pathological benchmarks for diagnosis and future research.

Keywords

Dromedary, Cirrhosis, Hepatic pathology, Immunohistochemistry, Morphometry, Liver

1. Introduction

The dromedary camel (*Camelus dromedarius)* is an economically and culturally important livestock species well adapted to the arid and semi-arid environments of North Africa, including Algeria [1,2]. It serves as a major source of meat, milk, and transport for rural communities. The liver, being central to metabolism, detoxification, and synthesis, plays a crucial role in maintaining animal health and productivity.

Hepatic pathology in dromedary camels has significant economic consequences as liver lesions often cause partial or total organ condemnation at slaughterhouses and chronic liver disease can impair growth, productivity, and carcass quality,

ultimately affecting local and international camel trade [3].

Hepatic cirrhosis represents the terminal stage of chronic liver injury, characterized by irreversible replacement of hepatic parenchyma by fibrous tissue and the formation of regenerative nodules [4,5]. While this condition has been extensively studied in humans and common domestic animals, its occurrence and pathological characteristics in camels remain poorly documented [6,7]. In camels, several factors have been suggested as possible causes of chronic hepatic damage, including parasitic infections such as hydatidosis and fascioliasis [8,9], exposure to hepatotoxic plants and mycotoxins, as well as nutritional imbalances [10,11].

These insults trigger the activation of hepatic stellate cells, which transform into α-smooth muscle actin (α-SMA)–positive myofibroblasts, leading to excessive extracellular matrix deposition and fibrosis [12].

From a pathogenic perspective, hepatic fibrosis is driven by the interaction between inflammatory cells and fibrogenic effector cells. CD68-positive macrophages play a central role by releasing pro-fibrotic cytokines, while activation of hepatic stellate cells into α-SMA–positive myofibroblasts represents the main source of extracellular matrix deposition [13].

Despite the suspected importance of chronic liver diseases in camel health, comprehensive pathological descriptions and quantitative data are lacking. The present study was therefore designed to characterize hepatic cirrhosis in Algerian dromedary camels through a combination of gross pathology, morphometric analysis, histochemical evaluation, and Immunohistochemical assessment. This approach aimed to establish objective diagnostic criteria and provide reference data for future veterinary investigations.

2. Materials and Methods

2.1 Study Design and Sampling Site

A cross-sectional study was conducted between January 2022 and January 2024 at the municipal abattoir of El Oued Province, southeastern Algeria, a region with an arid Saharan climate. Liver specimens were collected post-slaughter from 48 adult dromedary camels *(Camelus dromedarius)* aged between five (5) and 12 years of both sexes. The control group (n = 24) consisted of livers without visible gross lesions, while the cirrhotic group (n = 24) included livers with macroscopic alterations consistent with cirrhosis, such as nodularity, firmness, and discoloration.

Livers were classified as cirrhotic based on the presence of diffuse fibrous septa forming regenerative nodules, disruption of normal lobular architecture, and associated macroscopic alterations such as nodularity and firmness. Samples showing limited fibrous expansion without nodule formation or architectural distortion were not included in the cirrhotic group. All samples were obtained during routine meat inspection procedures, and therefore no specific ethical approval was required. Each liver was photographed and weighed using a precision electronic balance.

2.2 Gross Examination

Gross examination included assessment of liver color, surface features (nodularity, capsular thickening, adhesions), consistency, associated lesions (e.g., parasitic cysts), and finally liver mass. Liver mass was measured using a precision electronic balance (±1 g accuracy). Representative tissue samples (≈1 cm^3) were taken from each liver, fixed in 10% neutral buffered formalin for at least 72 h, processed using the routine paraffin embedding technique, and sectioned at 4–5 µm.

Gross examination was performed according to standard veterinary pathological criteria as previously described by [14].

2.3 Histological and Immunohistochemical Analysis

Histochemical staining with hematoxylin and eosin (H&E) and Azan trichrome was performed following the manufacturers' standard protocols (Merck, Darmstadt, Germany). Briefly, deparaffinized sections were rehydrated through graded alcohols, stained with hematoxylin for 5 min, differentiated, counterstained with eosin for 2 min, dehydrated, and mounted. Azan trichrome staining was performed according to the

manufacturer's instructions for collagen visualization.

Immunohistochemistry was performed using a mouse monoclonal anti-CD68 antibody (clone KP1, Dako, Denmark; dilution 1:100) and a mouse monoclonal anti-α-smooth muscle actin antibody (clone 1A4, Dako, Denmark; dilution 1:200). Sections were incubated with primary antibodies overnight at 4°C. Detection was carried out using a streptavidin–biotin peroxidase system with diaminobenzidine (DAB) as chromogen.

2.4 Histomorphometric analysis

Quantitative histomorphometric analysis was performed to assess the relative composition of liver tissue. Digital photomicrographs of H&E-stained sections were captured at 200× magnification using a light microscope equipped with a digital camera (Olympus BX51, Olympus Corporation, Tokyo, Japan) and analyzed using ImageJ software (National Institutes of Health, USA), and the underlying structures were classified as hepatocytes, connective tissue, blood vessels/sinusoids, or bile ducts/ductules.

The volume density (Vv) was calculated as:
Vv = (Number of points hitting the structure / Total number of points) × 100.
The methodology followed the approach described by Avtondilov [15].

Digital photomicrographs were analyzed using calibrated morphometric software. All slides were independently evaluated by two observers blinded to group allocation.

2.5 Statistical Analysis

All statistical analyses were performed using IBM SPSS Statistics v26.0. Data for liver mass and morphometric parameters are expressed as mean ± standard deviation (SD). The normality of distribution was assessed using the Shapiro–Wilk test. Differences between the control and cirrhotic groups were analyzed using an independent samples Student's t-test. If normality assumptions were not met, the Mann–Whitney U test was applied as a non-parametric alternative. All statistical tests were two-tailed.

Differences were considered statistically significant at $p < 0.05$, with highly significant differences indicated at $p < 0.01$ and $p < 0.001$.

3. Results

3.1 Macroscopic Findings

Gross examination revealed distinct differences between healthy and cirrhotic livers. Healthy livers exhibited a characteristic dark brown color, a smooth capsular surface, and a soft, uniform consistency, with no associated lesions (Fig. 1A). In contrast, cirrhotic livers showed discoloration, a markedly nodular surface architecture ranging from micronodular to macronodular patterns, firm to hard consistency upon palpation, and occasional associated lesions such as parasitic cysts (Fig. 1B).

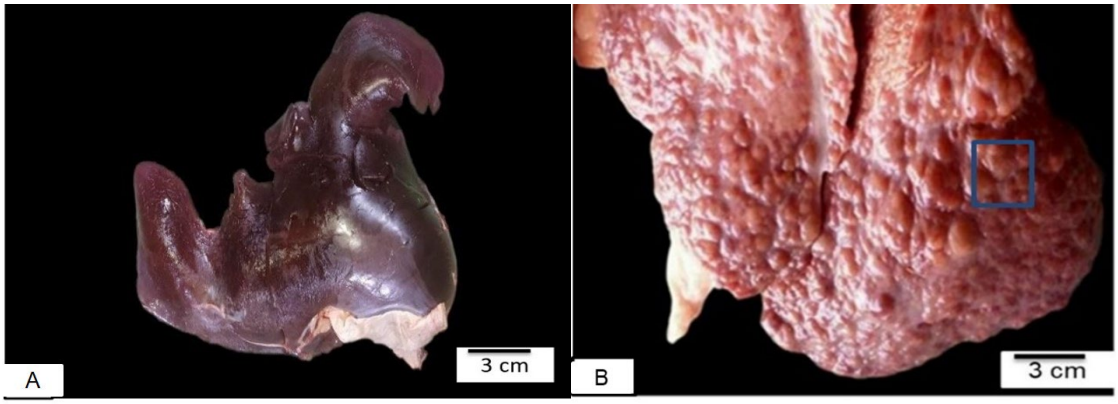

Figure 1. Macroscopic comparison: Healthy liver (A) and macronodular cirrhotic liver (B) of a dromedary camel *(Camelus dromedarius)* from the El Oued Region.

Macroscopic lesions in cirrhotic livers were predominantly concentrated in the peripheral regions of the hepatic parenchyma, with nodules extensively involving the subcapsular and peripheral areas of the liver lobes. Fibrotic changes were pronounced in these peripheral zones and extended inward, resulting in severe and generalized architectural distortion.

No significant differences in age range or sex distribution were observed between the control and cirrhotic groups.

Quantitative analysis confirmed a significant reduction ($p < 0.01$) in the mean mass of cirrhotic livers (6.30 ± 1.25 kg) compared to the healthy control group (8.12 ± 1.86 kg), representing a mean mass loss of approximately 22.41% (Table 1).

3.2 Histopathological Findings

Histological examination of healthy livers revealed a well-preserved lobular architecture. Hepatocytes were organized in regular radial plates extending from the central vein, with intact hepatic sinusoids interposed between the hepatocellular cords. The hepatocytes exhibited a polygonal morphology with homogeneous cytoplasm and centrally located nuclei, without evidence of cellular degeneration, necrosis, fibrosis, or inflammatory infiltration. Portal tracts appeared unremarkable, confirming the structural integrity of the hepatic parenchyma. At low magnification, the liver tissue displayed a homogeneous appearance with preserved lobular organization and an absence of fibrous septa or regenerative nodules, consistent with normal histological architecture (Fig. 2A and 2B).

Table 1**.** Morphometric comparison of liver mass (mean ± SD) between healthy and cirrhotic dromedary camels.

Characteristic	Minimum (kg)	Maximum (kg)	Mean ± SD (kg)	p-value
Healthy liver mass	5.50	10.27	8.12±1.86	
Cirrhotic liver mass	4.20	8.75	6.30±1.25**	0.008

Values are expressed as mean ± SD. Statistical significance: *p < 0.05; ** p < 0.01; *** p < 0.001.

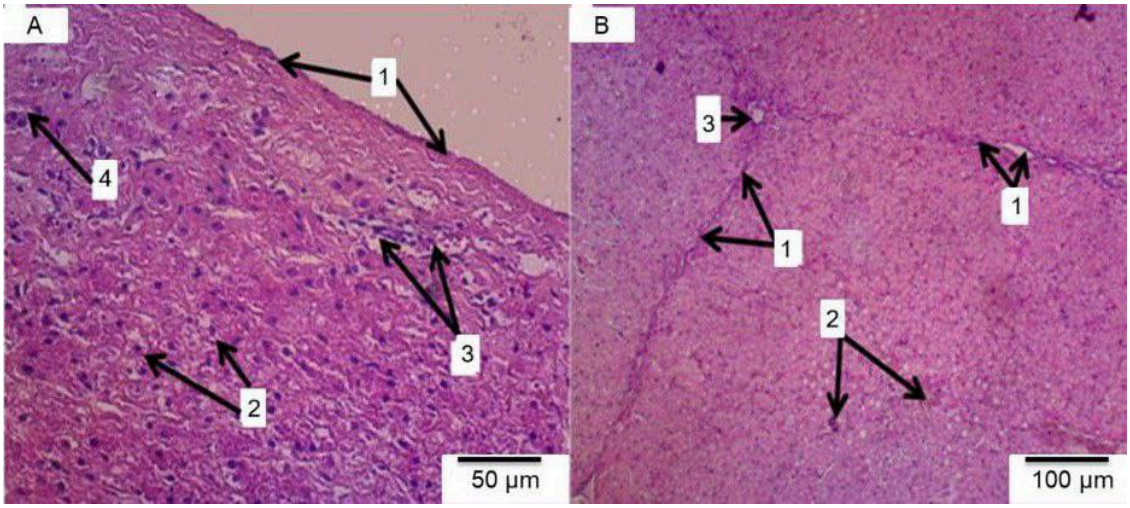

Figure 2. Histological section of a healthy dromedary liver, H&E staining, A: 1- Glisson's capsule; 2- hepatocytes, 3- hepatic sinusoids; 4- Kupffer cells, X400. B: 1- interlobular connective tissue, 2- hepatocytes, 3- central vein, X100.

In cirrhotic livers, the normal hepatic architecture was completely disrupted. Figure 3 illustrates cirrhotic dromedary liver tissue stained with Azan trichrome. At higher magnification (Fig. 3A), thick collagen-rich fibrous septa intensely stained blue are observed extensively subdividing the hepatic parenchyma. These septa contain proliferating bile ducts and small vascular structures and exert compressive effects on the adjacent hepatic tissue, consistent with advanced fibrotic remodeling. At lower magnification (Fig. 3B), a well-defined regenerative nodule is evident, surrounded by dense fibrotic bands. The fibrous septa are associated with inflammatory cell infiltrates and vascular elements, reflecting marked architectural distortion characteristic of established hepatic cirrhosis.

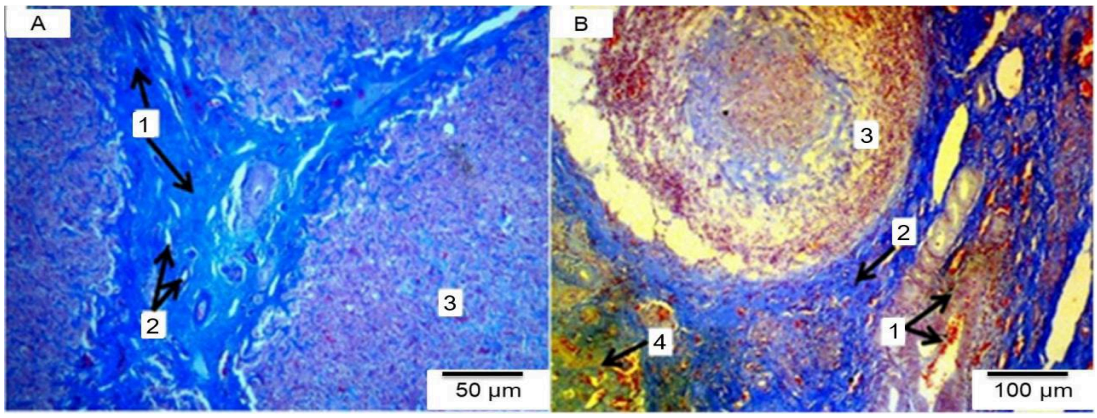

Figure 3. Histological section of dromedary liver tissue, affected by hepatic cirrhosis, Azan trichrome staining, A: 1- Fibrous septa; 2- Blood vessels; 3- Hepatic parenchyma, X400. B: 1- Blood vessels; 2- Fibrous tissue; 3- regeneration nodules; 4- Inflammatory infiltrate, X100.

3.3 Immunohistochemical Findings

In cirrhotic livers, α-SMA immunoreactivity was intensely localized within numerous elongated, spindle-shaped cells distributed along thick fibrous septa. Strong brown cytoplasmic DAB staining was observed in cells embedded within densely collagenized connective tissue and arranged parallel to fibrotic bands, whereas surrounding hepatocytes exhibited minimal to no immunoreactivity (Fig. 4A). CD68 immunostaining revealed numerous positively stained macrophages predominantly localized within septal inflammatory infiltrates and peri-nodular regions. These CD68-positive cells appeared either individually dispersed or clustered within fibrotic areas (Fig. 4B).

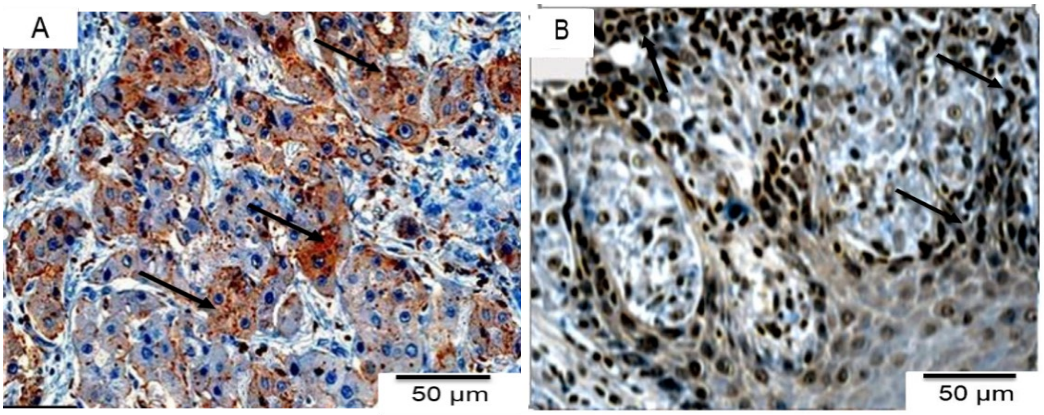

Figure 4. Immunohistochemical staining of hepatic parenchyma from dromedary camels with hepatic cirrhosis (×400). A: positive staining with α-SMA antibody . B: positive staining with CD68 antibody.

The spatial colocalization of activated stellate cells and macrophages within fibrotic septa underscores their coordinated contribution to sustained extracellular matrix deposition and progressive architectural remodeling. Collectively, these immunohistochemical findings confirm the pivotal and synergistic involvement of hepatic stellate cells and macrophages in the pathogenesis and progression of camel hepatic cirrhosis.

3.4 Histomorphometric analysis

The point-counting morphometric analysis provided quantitative data on the extensive tissue remodeling observed in cirrhotic livers (Table 2). The most pronounced change was a greater than 4.5-fold expansion of connective tissue, which increased from 7.25 ± 2.65% in healthy livers to 33.25 ± 2.31% in cirrhotic livers ($p < 0.001$). Concurrently, the proportion of functional hepatocytes was markedly reduced from 82.64 ± 4.87% to 54.34 ± 4.24% in cirrhotic livers ($p < 0.001$). Smaller but statistically significant increases were also observed in the vascular (blood vessels and sinusoids) and biliary compartments ($p < 0.05$).

Table 2. Histomorphometric composition (%) of hepatic tissue in healthy and cirrhotic dromedary camels.

Tissue Component	Healthy Liver (% ± SD)	Cirrhotic Liver (% ± SD)	p-value
Hepatocytes	82.64 ± 4.87	54.34 ± 4.24***	$p < 0.001$
Blood vessels + Sinusoids	9.57 ± 1.44	11.68 ± 2.05*	0.041
Bile ducts + Canaliculi	0.18 ± 0.12	0.41 ± 0.21*	0.032
Connective tissue	7.25 ± 2.65	33.25 ± 2.31***	$p < 0.001$

Values are expressed as mean ± SD. Statistical significance: *$p < 0.05$; ** $p < 0.01$; *** $p < 0.001$.

4. Discussion

This study provides the first comprehensive histopathological and histomorphometric characterization of hepatic cirrhosis in the dromedary camel, a disease of considerable economic and animal welfare relevance in arid regions. The observed pathological features are broadly consistent with the established mechanisms of cirrhosis described in other species, while also reflecting aspects that may be particularly relevant to camel physiology [16].

The most prominent gross alteration was the significant reduction in liver mass (approximately 22%) in cirrhotic animals, as demonstrated in the present study. Such hepatic atrophy is a characteristic feature of advanced cirrhosis and results from progressive loss of functional hepatocytes and their replacement by dense fibrous tissue [17]. The nodular surface and increased firmness observed macroscopically directly correspond to the microscopic processes of regenerative nodule formation and fibrotic septation.

Histologically, the complete disruption of normal lobular architecture and its subdivision into regenerative nodules by broad fibrous septa represent the defining hallmarks of cirrhosis [15]. The associated ductular proliferation and mononuclear inflammatory infiltrates observed within fibrous septa reflect a chronic reparative response to sustained hepatic injury, a pattern commonly reported in chronic liver diseases across species [18,19].

The severity of these structural alterations was objectively confirmed by quantitative histomorphometric analysis. Connective tissue content increased more than 4.5-fold in cirrhotic livers, while hepatocyte volume density decreased markedly from approximately 82% to 54%. This quantitative shift provides a robust and objective measure of parenchymal loss and functional compromise, reinforcing the advanced stage of disease in the examined animals [20].

Immunohistochemical findings, interpreted qualitatively rather than quantitatively, further elucidated the cellular mechanisms underlying fibrogenesis. The marked expansion of α-SMA-positive myofibroblasts within fibrous septa confirms the activation of hepatic stellate cells,

which are universally recognized as the principal source of pathological collagen deposition in liver fibrosis [21]. Concurrently, the increased presence of CD68-positive macrophages indicates persistent inflammatory activity. These cells secrete profibrotic mediators such as transforming growth factor-ß and platelet-derived growth factor, which sustain stellate cell activation and perpetuate extracellular matrix accumulation [22].

The interaction between activated myofibroblasts and inflammatory macrophages likely establishes a self-perpetuating cycle of injury, inflammation, and fibrosis, accounting for the progressive and irreversible nature of cirrhosis [23]. Although similar pathogenic pathways have been described in other species, their demonstration in camels is of particular importance given the scarcity of detailed pathological data in this species.

From a species-specific perspective, the functional implications of these architectural changes may be especially pronounced in camels dromedary. The extensive replacement of hepatocellular parenchyma by fibrous tissue is expected to impair essential hepatic functions, including metabolism, detoxification, and protein synthesis. Considering the camel's physiological adaptation to prolonged nutritional and water stress in arid environments, such severe structural damage may remain clinically unapparent until advanced stages, potentially explaining delayed detection despite extensive histopathological lesions [24].

Conclusions

In conclusion, this study establishes a definitive histopathological and immunomorphometric profile of hepatic cirrhosis in dromedary camels. We have quantitatively demonstrated the replacement of functional parenchyma by fibrous tissue and identified the key cellular players such as activated myofibroblasts and macrophages that are involved in this process. These findings provide robust diagnostic criteria and quantitative benchmarks that will serve as a valuable tool for veterinary pathologists and clinicians in diagnosing and understanding the pathogenesis of chronic liver disease in this economically vital species.

Availability of Data and Materials

All data generated or analyzed during this study are included in this published article.

Author Contributions

Conceptualization, A.C.B.; Methodology, A.C.B.; Investigation, A.C.B.; Data Analysis, A.C.B.; Writing – Original Draft, A.C.B.; Review & Editing, D.E.R.; Supervision, D.E.R.

Ethics Approval and Consent to Participate

All samples were collected post-slaughter during routine meat inspection; hence no ethical approval was required.

Acknowledgment

The authors wish to express their gratitude to the staff who assisted in completing this work, particularly the engineers of the histology and anatomy laboratories at the Institute of Veterinary Sciences, Taoura University, Souk Ahras, Algeria.

Funding

This research received no external funding.

Conflict of Interest

The authors declare no conflict of interest.

References

[1] Yilmaz, O. (2018). Camel wrestling economy in modern Turkey. *International Journal of Livestock Research, 8*(1), 39–46. https://doi.org/10.5455/ijlr.20170923122953.

[2] Faye, B. (2013). Camel meat in the world. In I.T. Kadim, O. Mahgoub, B. Faye, & M.M. Farouk (Eds.), *Camel meat and meat products*. 7-16. CABI: UK. https://doi.org/10.1079/9781780641010.0007.

[3] Ahmed, N.I., Ahmed, A.M., & Abdel-Wahab, M.A. (2023). Hygienic, pathological and economic impacts of liver lesions at some slaughterhouses in Suez Canal Region, Egypt. *Journal of Advanced Veterinary Research, 13*(6), 1017–1021.

[4] Koyama, Y., & Brenner, D.A. (2017). Liver inflammation and fibrosis. *Journal of Clinical Investigation, 127*(1), 55–64. https://doi.org/10.1172/JCI88881.

[5] Friedman, S.L. (2008). Mechanisms of hepatic fibrogenesis. *Gastroenterology, 134*(6), 1655–1669. https://doi.org/10.1053/j.gastro.2008.03.003.

[6] Al-Hizab, F.A., Hamouda, M.A., Amer, O.H., Edris, A.M., El-Ghareeb, W.R., Abdel-Raheem, S.M., Hawas, N., Elmoslemany, A.M., & Ibrahim, A.M. (2018). Cystic echinococcosis in dromedary camels: Biochemical, histopathological and parasitological studies. *Journal of Camel Practice and Research, 25*(2), 237–242. https://doi.org/10.5958/2277-8934.2018.00031.0.

[7] Mohammed, N., & Osman, H. (2016). Histopathological studies on liver affected with hydatidosis in one-humped camel (*Camelus dromedarius*) in Tampool slaughterhouse, Sudan. *Annual Research & Review in Biology, 11*(1), 1–6. https://doi.org/10.9734/ARRB/2016/28101.

[8] Abebe, N., Asrade, B., & Mekibib, B. (2021). Prevalence of cystic echinococcosis in one-humped camels slaughtered at Addis Ababa Municipality Abattoir, Ethiopia. *Ethiopian Veterinary Journal, 25*(1), 43–57. https://doi.org/10.4314/evj.v25i1.3.

[9] Asopa, S., Vyas, I., Dadhich, H., & Joshi, A. (2022). Pathological study of various liver lesions prevalent in camels of Rajasthan. *Journal of Camel Practice and Research, 29*(2), 223–228. https://doi.org/10.5958/2277-8934.2022.00031.5.

[10] Purohit, S., Malik, V., Gangwar, N.K., & Pandey, R.P. (2014). Diagnosis and surgical management of fibroma in a camel (*Camelus dromedarius*). *Journal of Camel Practice and Research, 21*(2), 275–278. https://doi.org/10.5958/2277-8934.2014.00048.4.

[11] Rahmoun, D.E., & Zeghdani, M.E.A. (2024). Castration and its effect on camel meat quality in El Oued, South Algeria. *Theoretical and Applied Veterinary Medicine, 12*(4), 16–20. https://doi.org/10.32819/2024.12018.

[12] Bedair Dewidar, C.M., Dooley, S., & Meindl-Beinker, N. (2019). TGF-ß in hepatic stellate cell activation and liver fibrogenesis—Updated 2019. *Cells, 8*(11), 1419. https://doi.org/10.3390/cells8111419.

[13] Wang, Z., Dong, S., & Zhou, W. (2024). Pancreatic stellate cells: Key players in pancreatic health and diseases. *Molecular Medicine Reports, 30*(1), 109. https://doi.org/10.3892/mmr.2024.13233.

[14] Munro, R., & Munro, H.M.C. (2013). Some challenges in forensic veterinary pathology: A review. *Journal of Comparative Pathology*, 149(1), 57–73. https://doi.org/10.1016/j.jcpa.2012.10.001.

[15] Avtandilov, G.G. (1990). *Medical morphometry*: A guide. Moscow: Medicine.

[16] Tharwat, M. (2020). Ultrasonography of the liver in healthy and diseased camels. *Journal of Veterinary Medical Science, 82*(4), 399–407. https://doi.org/10.1292/jvms.19-0690.

[17] Abdu, S.B. (2018). A new perspective in liver fibrosis: Etiology removal does not cause regression of liver fibrosis. *Journal of Histology and Histopathology, 5*(1), 6. https://doi.org/10.7243/2055-091x-5-6.

[18] Tsuchida, T., & Friedman, S.L. (2017). Mechanisms of hepatic stellate cell activation. *Nature Reviews Gastroenterology & Hepatology, 14*(7), 397–411. https://doi.org/10.1038/nrgastro.2017.38.

[19] Ferrell, L. (2000). Liver pathology: Cirrhosis, hepatitis, and primary liver tumors. Update and diagnostic problems. *Modern Pathology, 13*(6), 679–704. https://doi.org/10.1038/modpathol.3880119.

[20] Fuchs, B.C., Hoshida, Y., Fujii, T., Wei, L., Yamada, S., Lauwers, G.Y., & Tanabe, K.K. (2014). Epidermal growth factor receptor inhibition attenuates liver fibrosis and development of hepatocellular carcinoma.

Hepatology, *59*(4), 1577-1590. https://doi.org/10.1002/hep.26898.

[21] Lopez-Lopez, V., Linecker, M., Caballero-Llanes, A., Reese, T., Oldhafer, K.J., Hernandez-Alejandro, R., & Robles-Campos, R. (2024). Liver histology predicts liver regeneration and outcome in ALPPS: Novel findings from a multicenter study. *Annals of Surgery*, *279*(2), 306-313. https://doi.org/10.1016/j.hpb.2024.03.238.

[22] Tacke, F., & Zimmermann, H.W. (2014). Macrophage heterogeneity in liver injury and fibrosis. *Journal of Hepatology*, *60*(5), 1090-1096. https://doi.org/10.1016/j.jhep.2013.12.025.

[23] Van Beuge, M.M., Prakash, J., Lacombe, M., Post, E., Reker-Smit, C., Beljaars, L., & Poelstra, K. (2013). Enhanced effectivity of an ALK5-inhibitor after cell-specific delivery to hepatic stellate cells in mice with liver injury. *PloS One*, 8(2), e56442. https://doi.org/10.1371/journal.pone.0056442.

[24] El-Hady, E., Behairy, A., Goda, N. A., Abdelbaset-Ismail, A., Ahmed, A.E., Al-Doaiss, A. A., & Aref, M. (2023). Comparative physiological, morphological, histological, and AQP2 immunohistochemical analysis of the Arabian camels (*Camelus dromedarius*) and oxen kidney: Effects of adaptation to arid environments. *Frontiers in Animal Science*, *4*, 1078159. https://doi.org/10.3389/fanim.2023.1078159.